Cellular Responses to Patterned Poly(acrylic acid) Brushes

ARTICLE *in* LANGMUIR · JUNE 2011

Impact Factor: 4.46 · DOI: 10.1021/la200093e · Source: PubMed

Published in final edited form as:
Langmuir. 2011 June 7; 27(11): 7016–7023. doi:10.1021/la200093e.

Cellular Responses to Patterned Poly(Acrylic Acid) Brushes

Ethan N. Chiang[1], **Rong Dong**[1], **Christopher K. Ober**[2,*], and **Barbara A. Baird**[1]

[1]Department of Chemistry and Chemical Biology, Baker Laboratories, Cornell University, Ithaca, NY 14853

[2]Department of Materials Science and Engineering, Bard Hall, Cornell University, Ithaca, NY 14853

Abstract

We use patterned poly(acrylic acid) (PAA) polymer brushes to explore the effects of surface chemistry and topography on cell-surface interactions. Most past studies of surface topography effects on cell adhesion have focused on patterned feature sizes that are larger than the dimensions of a cell, and PAA brushes have been characterized as cell repellent. Here we report cell adhesion studies for RBL mast cells incubated on PAA brush surfaces patterned with a variety of different feature sizes. We find that when patterned at sub-cellular dimensions on silicon surfaces, PAA brushes that are 30 or 15 nm thick facilitate cell adhesion. This appears to be mediated by fibronectin, which is secreted by the cells, adsorbing to the brushes and then engaging cell surface integrins. The result is detectable accumulation of plasma membrane within the brushes, and this involves cytoskeletal remodeling at the cell-surface interface. By decreasing brush thickness, we find that PAA can be 'tuned' to promote cell adhesion with down-modulated membrane accumulation. We exemplify the utility of patterned PAA brush arrays for spatially controlling the activation of cells by modifying brushes with ligands that specifically engage IgE bound to high affinity receptors on mast cells.

Introduction

In living systems the interactions that occur between the plasma membrane of cells and the extracellular matrix (ECM) determine cell adhesion, motility, growth, segregation between tissues, and other responses. In translational applications such as biomedical implantation, tissue engineering and cell-based sensors, successful interfacing of materials and devices with biological systems requires an accurate assessment of cellular responses to a particular substrate's surface chemistry and topography. Information about these interactions, which occur on cellular and subcellular length scales, provides the key for tuning the biocompatibility of surface materials.

Recently, polymer brushes have attracted considerable attention for biofunctional modification of surfaces, due to their versatile chemistry and topography. Compared to self-assembled monolayers (SAMs), polymer brushes provide a higher density of functional groups, and they can be used, for example, to immobilize multiple layers of proteins[1] and generate protein arrays [2]. The thickly branched structure of hydrophilic polymer brushes in aqueous solutions are more likely than SAMs to mimic the ECM environment as it is presented *in vivo*.

Previous studies investigating surface chemistry and topography effects on cell adhesion have typically employed uniform surfaces or patterned features with dimensions larger than

CORRESPONDING AUTHOR FOOTNOTE: Phone: 607-255-8417; Fax: 607-255-2365; cko3@cornell.edu.

those of a cell (≫10μm)[3; 4; 5]. Here we report distinctive responses of RBL mast cells that are incubated on patterned poly (acrylic acid) (PAA) brush surfaces with variable thickness and feature sizes ranging from micrometers to hundreds of micrometers. Various cell types under various conditions have different propensities to stick to a particular surface as determined by cell membrane properties and the possibly by cellular secretions that modulate these interactions. We chose RBL cells for our study because they adhere readily to glass or silicon surfaces, mediated in part by secretion of fibronectin that adsorbs to these surfaces and binds to cell surface intergrin receptors[6]; [7]. We evaluated adherence of RBL cells to PAA brushes of various designs as compared to bare silicon surfaces. We find that PAA brushes that typically repel adhesion of these cells, promote fibronectin-mediated cell adhesion when patterned at sub-cellular dimensions. Moreover, the plasma membrane accumulation that occurs within the brushes under these conditions can be modulated by adjusting polymer brush thickness. We demonstrate that patterned PAA arrays can be covalently modified with specific ligands for cell surface receptors, and this provides a spatially controlled means of activating cells. In particular, we show that mast cell signaling can be investigated with patterned features of PAA conjugated with 2,4 dinitrophenyl (DNP) groups that specifically bind and cluster anti-DNP IgE bound to high affinity cell surface receptors FcεRI.

Experimental

Materials

Allyl 2-bromo-2-methylpropionate, chlorodimethylhydrosilane, Pt on activated carbon (10 wt %), triethylamine, CuBr, $CuBr_2$, 2,2′-bipyridine, sodium acrylate, diisoproplycarbodiimide (DIPC), and all solvents used were purchased from Sigma-Aldrich. All chemicals were used without further purification. Distilled deionized (DI) water and high-purity nitrogen gas (99.99 %, Airgas) were used in synthetic procedures throughout. Silicon wafers covered with native silicon oxide layer were purchased from Montco Silicon Technologies. Surface initiator for silica substrates was synthesized and immobilized to substrates as described below. 4-(dimethylamino)pyridinium-4-toluenesulfonate (DPTS) was synthesized according to a literature procedure[8]. A488-IgE was prepared by modification of purified mouse monoclonal anti-DNP IgE with Alexafluor 488 (A488; Invitrogen) as previously described[9]. A488 cholera toxin subunit B, 1,1’-dihexadecyl-3,3,3’, 3’-tetramethylindocarbocyanine perchlorate ($DiIC_{16}$) and 1,2- dipalmitoyl-*sn*-glycero-3-phospho-ethanol-amine-x-Texas red (TR-DPPE) were purchased from Invitrogen. Cytochalasin D was purchased from Sigma-Aldrich, and RGD peptides were purchased from Calbiochem. Actin-EGFP was a gift from A. Jeromin (Allen Institute, Seattle, WA).

Patterning and Synthesis of PAA Brushes on Silicon Surfaces

PAA brushes were patterned on silicon surfaces using a photolithography procedure, which is depicted in Figure 1 using a procedure described elsewhere [2]. Briefly, a layer of lift-off photoresist 5A (LOR 5A) was spin-coated onto a silicon wafer prior to performing photolithography. The photoresist was processed using standard procedures. After patterning and surface cleaning, initiator (3-(chlorodimethylsilyl)propyl 2-bromo-2-methylpropionate) was attached to the exposed silicon oxide surface, followed by surface-initiated ATRP polymerization of sodium acrylate in water (for 2h at 37°C). PAA brushes with different thicknesses (30 nm to 8 nm) were prepared by varying the monomer concentrations in the polymerization media (1.88 g sodium acrylate dissolved in 4, 5 or 6 mL of DI water). After growth of the resulting poly(sodium acrylate) brush to the proper thickness, the LOR 5A was subsequently removed. A buffer was used to convert the salt form of the brush to the poly(acrylic acid), PAA, form. The dimensions of the patterned PAA brushes were

determined using atomic force microscopy (AFM), and brush thicknesses were determined with AFM and ellipsometry.

Synthesis of PAA Brushes modified with DNP groups (DNP-PAA)

Patterned PAA brush surfaces were prepared, as described above, except that shorter polymerization times (~20 min) were used. N, N'-2,4-DNP-ε-amino-caproate conjugated to poly(ethylene) glycol (DNP-PEG) was synthesized as previously reported[10] and attached to the patterned PAA brushes via hydroxyl moieties, as shown in Figure 2. Briefly, patterned PAA substrates were placed in a 25 mL Schlenk flask containing 75 mg of DPTS. Following evacuation and back-filling with nitrogen three times, 4 mL anhydrous dichloromethane was added to the flask using a cannula. After the DPTS completely dissolved, 0.05 mL DNP-PEG and 0.05 mL DIPC were added to the reaction mixture, and the solution was reacted overnight at room temperature. The patterned PAA-DNP substrates were then rinsed with water and isopropanol, blown dry, and stored in the dark prior to use for cell experiments. X-ray Photoelectron Spectroscopy (XPS) was used to confirm attachment of DNP to PAA by monitoring the appearance of a nitrogen peak in the XPS spectrum.

RBL Cells Interactions with Patterned Brush Surfaces

RBL-2H3 cells were maintained in tissue culture and harvested as previously described[9]. After 1 hr of sensitization with A488-IgE (1 μg/mL), cells were washed and incubated on patterned substrates (at a concentration of 0.5×10^6 cells/mL) at either 37°C or room temperature for 20 min. These substrates were gently rinsed with buffered saline solution (BSS: 150 mM NaCl, 2.5 mM KCl, 12 mM $NaHCO_3$, 2 mM glucose, pH 7.4) to remove $MgCl_2$, 2 mML $CaCl_2$, 1 mg/mL bovine serum albumin, 1 mg/mL unattached cells. The substrates were then placed in MatTek dishes filled with BSS and imaged using confocal fluorescence microscopy. For most experiments, cells on the substrates were visualized with A488-IgE bound to cell surface receptors FcεRI. In some cases, cell membranes were labeled with either 2 μg/mL A555-CTxB, 10 μM TR-DPPE, or 10 μM $DiIC_{16}$, which typically labeled >80% of all cells. Membrane markers were added to suspended cells for 5 min at room temperature, and cells were washed prior to incubation on patterned substrates. RBL cells expressing actin-EGFP were prepared using standard transfection procedures, as previously described [7].

Fibronectin-coated Surfaces

In some experiments patterned substrates were incubated with 50 μg/mL bovine fibronectin for 1 hr at 37°C and then rinsed with BSS to remove fibronectin that was not strongly adsorbed to the surface. Fibronectin distributions were visualized with confocal microscopy after immunofluorescence labeling (anti-fibronectin mAb followed by A555-labeled goat anti-mouse pAb) using standard procedures[7].

Treatments with Cytochalasin D and RGD Peptides

Suspended cells were treated with 1 μg/mL cytochalasin D in BSS for 10 min at 37°C prior to incubation on the patterned PAA substrates (in continued presence of cytochalasin D) for 20 min at 37°C. In drug-washout experiments, the BSS+cytochalasin D solution was replaced with fresh BSS, and cell-substrates continued incubation at 37°C for 20 min. Identical concentrations and incubation times were used to treat cells-substrates with cytochalasin D post-incubation only. To inhibit integrin receptor binding, RBL cells were pre-treated with 1 μg/mL RGD peptides for ~30 min at 37°C prior to incubation on the patterned PAA substrates.

Confocal Fluorescence Microscopy

Images of fluorescently labeled RBL cells on patterned PAA surfaces were obtained with a Leica TCS SP2 confocal microscope at room temperature. A 40x 0.8 NA, long working distance, water immersion lens was used for image acquisition. Reflectance images were acquired using a highly attenuated laser to visualize the polymer brush pattern borders. For visualization purposes when necessary, grid lines were generated using these reflectance images and superimposed over cellular fluorescence images so that co-localization of cellular fluorescence with the underlying PAA brush patterns could be clearly identified (Figures 6, 8, 9, 10).

Results

Patterned PAA brush surfaces promote cell adhesion

Because of their tendency to adhere to bare surfaces and their biological relevance we used RBL mast cells as a model system[3]; [11]. We evaluated cell adherence to silicon surfaces patterned with PAA in the following features: strips with widths of 100 μm or 20 μm and squares with dimensions of 10 μm or 2 μm (Figure 1). The standard PAA thickness was 30 nm. RBL cells were labeled with A488-IgE bound to cell surface receptors, FcεRI, and incubated with each substrate for 20 min at 37°C before imaging with confocal fluorescence microscopy. Figure 3 shows representative images from these experiments. Figure 4 compares quantitatively cell adherence to silicon surfaces that are bare, uniformly modified with PAA brushes, or patterned with PAA brushes (2 μm square PAA features, 2μm pitch), as averaged over multiple experiments.

We found that RBL cells do not adhere to surfaces that are covered completely with PAA brushes, whereas these cells adhere readily to bare silicon surfaces (Figure 4). Similarly, when RBL cells are incubated on PAA surfaces patterned with 100 μm- or 20 μm-wide strips of alternating PAA brushes and silicon, cells adhere almost exclusively to silicon regions (Figures 3A, B). In both of these cases, patterned PAA feature dimensions are larger than those of the cells, and cells that happen to settle on the PAA brushes do not adhere. However, when patterned features are smaller than cellular dimensions, cells that settle on the PAA brushes also come into contact with the silicon surface. For cells incubated on surfaces patterned with 10 μm PAA squares, the majority of cells (~75%) adhere to bare silicon between the PAA regions. The remaining cells adhere mostly to silicon with partial membrane spreading over PAA brushes (Figure 3C). Cells incubated on surfaces patterned with 2 μm PAA squares necessarily come into contact with both silicon and PAA brushes and spread over both regions (Figure 3D), resulting in cell adherence comparable to that for bare silicon (Figure 4).

Membrane accumulates over patterned PAA brush regions at 37°C

Because cells typically avoid PAA brushes[3] (Figures 3, 4), we were surprised to find that for RBL cells adhering to the patterned substrates with 2 μm PAA squares, the plasma membrane markedly accumulates in the regions of the PAA (Figure 5). This membrane accumulation can be visualized by concentration of various fluorescent membrane markers: A488-IgE that binds to FcεRI (Figure 5A); A488-CTxB that binds to ganglioside GM1 (Figure 5C); TR-DPPE that partitions into the membrane lipid bilayer (Figure 5B). Similar membrane accumulation is observed when cells are incubated with substrates patterned with 2 μm and 5 μm strips of PAA brushes (data not shown), although cell densities on these surfaces were significantly lower (>50% reduction) than those observed with the 2 μm PAA squares.

To assess the role of cellular metabolism, we tested the effects of temperature on cell adherence and membrane accumulation over 2 μm PAA squares. Cells were labeled with A488-IgE and incubated at room temperature for 20 min, followed by a temperature shift to 37°C. When cells are incubated at room temperature only, <10% adhere to the patterned surface. Of the few cells that do adhere, the membrane does not accumulate significantly over the PAA features (Figure 6A). However, when the same sample of cells and substrate is incubated at 37°C for an additional 20 min, membrane accumulates markedly over PAA features (Figure 6B). If the sequence is reversed, and cells are initially incubated with substrates at 37°C (allowing membrane to accumulate over PAA features), then incubated at room temperature for additional 20 min, membrane accumulation over PAA regions is sustained (data not shown).

Membrane accumulation involves cell receptors binding to fibronectin

We investigated the mechanisms driving the cell-surface interactions at the membrane-brush interface. RBL cells are known to secrete the ECM protein fibronectin, which adsorbs to silicon and thereby facilitates cell adherence[7]. To determine whether PAA brushes adsorb and concentrate fibronectin, patterned PAA surfaces were incubated with 50 μg/mL soluble fibronectin for 1 hr at 37°C. Fibronectin distributions were labeled by immunofluorescence and visualized by confocal fluorescence microscopy. We find that fibronectin selectively accumulates over patterned PAA regions (Figure 7), and this is probably due to the substantially increased surface area provided by the brushes.

These results suggest that fibronectin secreted by cells that attach over the PAA regions is adsorbed to the brushes, then the cell membrane integrin receptors that bind fibronectin become localized in these regions, resulting in membrane accumulation. To reduce or eliminate integrin binding we employed Arginine-Glycine-Aspartate (RGD)-containing peptides derived from fibronectin that correspond to the integrin binding motif. Cells were incubated with RGD peptides (or BSS only) for 30 min at 37°C prior to incubation with surfaces patterned with 2 μm PAA squares. We found that pre-treatment with RGD peptides prevents the accumulation of membrane over PAA patterns. Under these conditions, cell adherence to the patterned PAA surfaces is also reduced (Figure 8).

Our results indicate that fibronectin-integrin binding is involved in membrane accumulation over PAA regions for cell attaching simultaneously to PAA and silicon surfaces on patterned subtrates. We investigated whether fibronectin adsorption to 100 μm wide lines of PAA (normally cell-repellent, Figure 3A) would facilitate cell adhesion. After confirming that fibronectin adsorbs and accumulates over 100 mm PAA regions with immunofluorescence (similar to Figure 7), cells were incubated with these fibronectin-treated surfaces for 20 min at 37°C. We found that cells still preferentially adhere to bare silicon (similar to Figure 3A), indicating that the presence of fibronectin alone is not sufficient to mitigate the cell-repellent nature of the PAA brushes. We find consistently that cell adherence requires some attachment to the silicon surface surrounding a PAA region. Collectively, our results suggest that localized membrane accumulation over PAA regions occurs through a two-step process where 1) cell adhesion usually only occurs if the patterned PAA features are small enough so that cells are exposed to sufficient silicon surface area, and 2) attached cells secrete soluble fibronectin, which adsorbs to PAA regions and initiates fibronectin-integrin engagement over PAA regions that results in membrane accumulation.

Cytoskeletal Contributions to Membrane Accumulation

Actin polymerization and cytoskeletal remodeling are hallmarks of integrin activation[12], and we explored the role of actin in the recruitment of plasma membrane to PAA regions. Fluorescent actin-EGFP was endogenously expressed in cells after transient transfection,

and these cells were incubated on patterned PAA surfaces (2 μm squares) at room temperature for 20 min followed by an upward temperature shift to 37°C for an additional 20 min. At room temperature, actin-EGFP is uniformly distributed at the plasma membrane over both silicon and PAA regions (Figure 9A). However, there is a dramatic redistribution of actin-EGFP to PAA regions when the incubation temperature is increased to 37°C (Figure 9B). This temperature-dependent reorganization of actin to PAA regions parallels that of the fluorescent membrane markers visualized in Figure 6.

We investigated the effects of cytochalasin D, a drug that inhibits actin polymerization in RBL cells[6], on plasma membrane accumulation over PAA patterned in 2μm squares. When A488-IgE sensitized cells are pre-treated with cytochalasin D for 10 min at 37°C and then incubated with substrates for 20 min at 37°C, membrane does not accumulate over PAA regions (Figure 10A). After subsequent wash-out of cytochalasin D and re-incubation at 37°C for 20 min, membrane accumulates over PAA regions (Figure 10B). If the sequence is reversed and cells are incubated on patterned PAA surfaces for 20 min at 37°C (Figure 10C) prior to treatment with cytochalasin D (Figure 10D), the accumulation of membrane over PAA regions is sustained. These results indicate that localized polymerization of actin initiates the recruitment of membrane to PAA regions, but that sustained membrane accumulation over PAA does not require continuing actin polymerization.

Tuning membrane accumulation by varying polymer brush thickness

Our standard PAA brush thickness for experiments described above (Figures 3 - 10) was 30 nm, and we consistently observed cell membrane accumulation when PAA features were 2μm squares with cell incubation at 37°C under standard conditions (e.g., Figure 5). Brushes as thick as 50 nm were also investigated and also showed the effect. Brushes of greater thickness were not explored, because the uniformity and quality of the brushes becomes less reliable beyond that thickness. We hypothesized that the topographical depth of the PAA brushes influences cell adhesion, and we explored how this property affects the membrane accumulation. To make this comparison, we synthesized PAA brushes with reduced thicknesses (15 nm and 8 nm). A488-IgE labeled cells were incubated for 20 min at 37°C on surfaces with PAA patterned in 2 μm squares but with varying brush thicknesses. We found that the plasma membrane strongly accumulates over 30 nm (Figure 11A) and 15 nm (Figure 11B) thick PAA brushes. However, when PAA brush thickness is reduced to 8 nm, membrane does not accumulate visibly over PAA regions, yet cell adhesion (as quantified by cell density on substrates) is equivalent to that observed for 30 nm thick PAA surfaces with the same 2 μm features (Figure 11C). It should be noted that Figure 11C is taken at a lower magnification so that a larger field of view is possible.

While destructive interference present in a thin brush film could also reduce fluorescence signal, the cell membrane is known to be highly irregular over the scale of nanometers such that destructive interference is unlikely. To avoid being misled by possible optical effects, we made direct comparisons in all of our fluorescence imaging experiments. The differences in fluorescence observed over the patterned PAA features in each case cannot be easily explained by a consistent optical artifact and can be best explained by the relative capacity of the cell membrane, under specified experimental manipulation, to extend into the polymer brushes and thereby increase fluorescently labeled membrane surface area within the confocal plane of signal detection.

Patterned PAA-DNP arrays for spatially restricting IgE-FcεRI signaling—After establishing that PAA brush thickness can be tuned to eliminate membrane accumulation, we investigated the utility of these surfaces as versatile arrays for studying specific cell-surface interactions. We previously showed that patterned lipid bilayers[6] and SAMs[13]

containing specific ligands are valuable for investigating spatial regulation of IgE-receptor mediated mast cell signaling. Similarly, we investigated whether patterned PAA surfaces could be conjugated with DNP-ligands that selectively bind to anti-DNP IgE bound to FcεRI on RBL cells. We prepared patterned PAA-DNP ligand arrays by chemically functionalizing thin (~8 nm) patterned PAA brushes (2 μm square features) with DNP-PEG (Figure 2). Incorporation of a PEG linker reduces non-specific interactions between the substrate and other proteins and provides flexibility to the DNP-brushes in cell suspensions. The PEG linker further provides DNP groups better accessibility to IgE antibody binding sites, which is necessary for robust binding and clustering of cell surface IgE-FcεRI[14].

After cells that are sensitized with A448-IgE (specific for DNP) are incubated on the patterned PAA-DNP surfaces for 20 min at 37° C, A488-IgE is clearly concentrated over the patterned regions (Figure 12A). The specificity of IgE-FcεRI redistribution to PAA-DNP was confirmed by double labeling cells with A488-IgE and the fluorescent lipid analogue, DiI-C_{16}. As expected, A488-IgE-FcεRI accumulates over PAA-DNP regions (Figure 12B), while DiI-C_{16} remains uniformly distributed over both silicon and PAA-DNP regions (Figure 12C). The lack of visual correlation between A488-IgE and DiIC_{16} (Figure 12D) demonstrates selective redistribution of IgE-FcεRI in response to these patterned PAA-DNP arrays, quite distinctive from the nonspecific membrane accumulation we observed with 30 nm thick PAA brushes (Figure 5).

DISCUSSION

The implantation of materials and devices into biological systems triggers surrounding cells and tissues to initiate cellular responses that may favor implant assimilation or promote rejection. The importance of assuring a material's biocompatibility is underscored by the increasing utilization of non-biological materials in clinical research and medicine (for example, over 800,000 hip replacement surgeries are performed annually worldwide[15]). For this reason, the ability to control interactions at the interface between non-biological materials and cells within host tissues is ardently pursued in biomedical engineering.

In vivo, cell membranes are typically surrounded by a highly porous meshwork of glycosaminoglycans and fibrous proteins, such as fibronectin and collagen, forming the ECM. Several techniques are commonly used to impart bio-mimetic properties to a material's surface, including: adsorption and covalent attachment of adhesion-promoting biomolecules[16], modulating surface topology[17], and modified surface chemistries[18]. Polymer brushes have gained increasing popularity over the last decade as a means of incorporating versatile functionality to a material's surface.

Of particular interest for the general utilization of PAA capacity is its capacity to act as a scaffold for immobilizing different biomolecules with specific cellular functions. Due to a high concentration of carboxylic acid groups (-COOH), unmodified PAA brushes have a strong capacity to adsorb proteins[19] and have thus been exploited as scaffolds for immobilizing collagen to enhance cell adhesion[20]. Additionally, PAA has been covalently modified with various proteins, demonstrating their utility as patterned protein arrays[2]. In this study, we used patterned PAA brushes to explore the effects of both surface chemistry and topography (pattern dimensions and thickness) on cell-surface interactions.

We chose RBL mast cells as a model system because they adhere readily to silicon and other surfaces. However, when RBL cells are incubated on surfaces that are uniformly modified with PAA, very few cells attach to these PAA brushes (Figure 4). This is consistent with previous reports that demonstrate PAA surface modification typically resists cell adhesion[21]. Consequently, it is not surprising that RBL cells incubated on PAA surfaces patterned at

large dimensions (larger than the size of a cell) preferentially adhere to bare silicon regions (Figure 3A-C). Interestingly, when PAA brushes are patterned at dimensions smaller than that of a cell (2 μm squares) we found that 1) cells attach and spread over both PAA and silicon regions (Figure 3D), and 2) cell membrane selectively accumulates over regions of PAA (30nm thick) at 37°C (Figure 5), and much less at room temperature (Figure 6). We also found that the accumulation of membrane over PAA regions is PAA brush thickness-dependent. In particular, we found that reducing brush thickness from 30 nm to 8 nm prevents membrane accumulation (Figure 11). We demonstrated that thin brushes can be used to concentrate selected cell surface receptors coinicident with patterned features by modifying the brushes with specific ligands (Figure 12). Such patterning of ligands has proved to be valuable for examining spatial regulation of receptor-mediated cell signaling[11].

In further examination of nonselective membrane accumulation with the thicker brushes, we showed that soluble fibronectin adheres and concentrates over patterned PAA regions (Figure 7). We hypothesized that RBL membrane accumulation is mediated by secreted fibronectin that interacts with receptors (integrins) on these cells. PAA brushes increase the surface area of the substrate affording more of these interactions, and this explanation is consistent with observed thickness-dependent membrane accumulation over PAA regions (Figure 11). Moreover, incubation in the presence of RGD peptides inhibits binding between cell integrins and fibronectin-rich PAA brushes, and the cell membrane does not accumulate over PAA regions under these conditions (Figure 8).

We believe that cells landing upon PAA surfaces do not attach because during the limited time of association insufficient quantities of fibronectin (and possibly other substances) are secreted. We suggest that these secreted substances must adhere at a sufficient density for effective engagement of integrin receptors and cell attachment. Therefore, during this limited time of association, cells will adhere much more readily to a silicon surface and not to the PAA brush areas, even if they are immediately adjacent. However, when the PAA brushes are surrounded by silicon, then the cells adhere to the silicon and continue to secrete fibronectin into the PAA brush areas. Under these circumstances, the density of adsorbed fibronectin becomes sufficient for effective integrin engagement and membrane penetration into the brushes (Figures 3D and 5).

One important consequence of multiple integrin engagement with fibronectin is rapid actin polymerization that accompanies localized cytoskeleton remodeling[22]. To test whether membrane redistribution to PAA regions is driven by integrin-dependent actin reorganization, we first confirmed that actin-EGFP accumulates over PAA regions (Figure 9). We then demonstrated that inhibiting actin polymerization with cytochalasin D prevents membrane accumulation over PAA regions (Figure 10A). Interestingly, while actin polymerization drives the formation of accumulated membrane structures over PAA regions, persistent actin polymerization is not required for sustained membrane association with PAA brushes (Figure 10D).

Many actin-rich membrane structures have been identified in cells, including membrane ruffles, protrusions, and podosomes, and these have been shown to play important roles in cell adhesion and motility, membrane trafficking and signaling. Despite diversity in protein composition and morphology, these structures provide common mechanisms for sensing, responding and interacting with their environment. We found that if constrained to lie over micron size features of PAA brushes, the RBL cells secrete fibronectin into them and then actively explore the interior surfaces. Previous studies showed that RBL cells extend filapodia like protrusions to investigate nanofabricated holes ~100 nm in diameter[23]. The polymerizing actin-driven membrane structures that interdigitate with the PAA brushes may

be related to invadopodia that have been implicated in tissue invasiveness and proteolytic ECM degradation[24]; [25].

Our study was partially motivated by a common practice in the field of biomaterials to use cell adhesion statistics to assess successful biocompatibility. Our observations with the PAA brushes clearly demonstrate that engineered surfaces can induce diverse cellular responses that depend on patterning morphology. Any particular response may or may not be desirable for a given application. The ability to generate cell- adhesive surfaces from cell-repellent materials using patterned surface morphologies may provide useful strategies for enhancing and fine-tuning the biocompatibility of other apparently resistive materials. In addition to regulating membrane interactions, the capacity to present biomolecules that specifically target cell surface receptors, demonstrates that PAA arrays are versatile substrates for engineering biological-materials interfaces for a wide variety of applications.

Acknowledgments

This work was funded in part by NIH grant AI018306 and by the Tri-Institutional Training Program in Chemical Biology. Partial support for this research came from the National Science Foundation through a grant administered by the Cornell Nanobiotechnology Center (NBTC) and from grant DMR-0518785. The authors acknowledge the use of the Cornell Nanoscale Facility and the use of the facilities of the Cornell NBTC.

References

1. Moore JS, Stupp SI. Room-Temperature Polyesterification. Macromolecules. 1990; 23:65–70.
2. Larson DR, et al. Temporally resolved interactions between antigen-stimulated IgE receptors and Lyn kinase on living cells. J Cell Biol. 2005; 171(3):527–36. [PubMed: 16275755]
3. Dong R, et al. Patterned biofunctional poly(acrylic acid) brushes on silicon surfaces. Biomacromolecules. 2007; 8(10):3082–92. [PubMed: 17880179]
4. Dong, R. Department of Chemistry and Chemical Biology. Cornell University; Ithaca: 2009. Synthesis, Characterization And Biological Applications Of Polyelectrolyte Brushes.
5. Baird EJ, et al. Highly effective poly(ethylene glycol) architectures for specific inhibition of immune receptor activation. Biochemistry. 2003; 42(44):12739–48. [PubMed: 14596588]
6. Wu M, et al. Visualization of plasma membrane compartmentalization with patterned lipid bilayers. Proc Natl Acad Sci U S A. 2004; 101(38):13798–803. [PubMed: 15356342]
7. Senaratne W, et al. Functionalized surface arrays for spatial targeting of immune cell signaling. J Am Chem Soc. 2006; 128(17):5594–5. [PubMed: 16637600]
8. Das R, et al. Binding mechanisms of PEGylated ligands reveal multiple effects of the PEG scaffold. Biochemistry. 2008; 47(3):1017–30. [PubMed: 18154361]
9. White LM, et al. Complications of total hip arthroplasty: MR imaging-initial experience. Radiology. 2000; 215(1):254–62. [PubMed: 10751496]
10. Altankov G, Grinnell F, Groth T. Studies on the biocompatibility of materials: fibroblast reorganization of substratum-bound fibronectin on surfaces varying in wettability. J Biomed Mater Res. 1996; 30(3):385–91. [PubMed: 8698702]
11. Kam L, et al. Correlation of astroglial cell function on micro-patterned surfaces with specific geometric parameters. Biomaterials. 1999; 20(23-24):2343–50. [PubMed: 10614940]
12. Keselowsky BG, Collard DM, Garcia AJ. Integrin binding specificity regulates biomaterial surface chemistry effects on cell differentiation. Proc Natl Acad Sci U S A. 2005; 102(17):5953–7. [PubMed: 15827122]
13. Dai J, et al. High-capacity binding of proteins by poly(acrylic acid) brushes and their derivatives. Langmuir. 2006; 22(9):4274–81. [PubMed: 16618175]
14. Bisson I, et al. Acrylic acid grafting and collagen immobilization on poly(ethylene terephthalate) surfaces for adherence and growth of human bladder smooth muscle cells. Biomaterials. 2002; 23(15):3149–58. [PubMed: 12102186]

15. Gupta B, et al. Plasma-induced graft polymerization of acrylic acid onto poly(ethylene terephthalate) films: characterization and human smooth muscle cell growth on grafted films. Biomaterials. 2002; 23(3):863–71. [PubMed: 11771705]
16. Lofgren R, et al. Beta 2 integrin engagement triggers actin polymerization and phosphatidylinositol trisphosphate formation in non-adherent human neutrophils. J Cell Biol. 1993; 123(6 Pt 1):1597–605. [PubMed: 7504676]
17. Bowden ET, et al. Co-localization of cortactin and phosphotyrosine identifies active invadopodia in human breast cancer cells. Exp Cell Res. 2006; 312(8):1240–53. [PubMed: 16442522]
18. Coopman PJ, et al. Integrin alpha 3 beta 1 participates in the phagocytosis of extracellular matrix molecules by human breast cancer cells. Mol Biol Cell. 1996; 7(11):1789–804. [PubMed: 8930900]
19. Linder S. The matrix corroded: podosomes and invadopodia in extracellular matrix degradation. Trends Cell Biol. 2007; 17(3):107–17. [PubMed: 17275303]
20. Stylli SS, Kaye AH, Lock P. Invadopodia: at the cutting edge of tumour invasion. J Clin Neurosci. 2008; 15(7):725–37. [PubMed: 18468901]
21. Moran-Mirabal, Jose M.; T, AJ.; Samiee, Kevan T.; Baird, Barbara A.; Craighead, Harold. Cell investigation of nanostructures: zero-mode waveguides for plasma membrane studies with single molecule resolution. Nanotechnology. 2007; (19)
22. Bengtsson T, et al. Actin dynamics in human neutrophils during adhesion and phagocytosis is controlled by changes in intracellular free calcium. Eur J Cell Biol. 1993; 62(1):49–58. [PubMed: 8269978]
23. Zhao MW, et al. A distinct integrin-mediated phagocytic pathway for extracellular matrix remodeling by RPE cells. Invest Ophthalmol Vis Sci. 1999; 40(11):2713–23. [PubMed: 10509670]
24. Everts V, et al. Phagocytosis and intracellular digestion of collagen, its role in turnover and remodelling. Histochem J. 1996; 28(4):229–45. [PubMed: 8762055]
25. Clark RA, Ghosh K, Tonnesen MG. Tissue engineering for cutaneous wounds. J Invest Dermatol. 2007; 127(5):1018–29. [PubMed: 17435787]
26. Senior RM, Griffin GL, Mecham RP. Chemotactic responses of fibroblasts to tropoelastin and elastin-derived peptides. J Clin Invest. 1982; 70(3):614–8. [PubMed: 7107897]

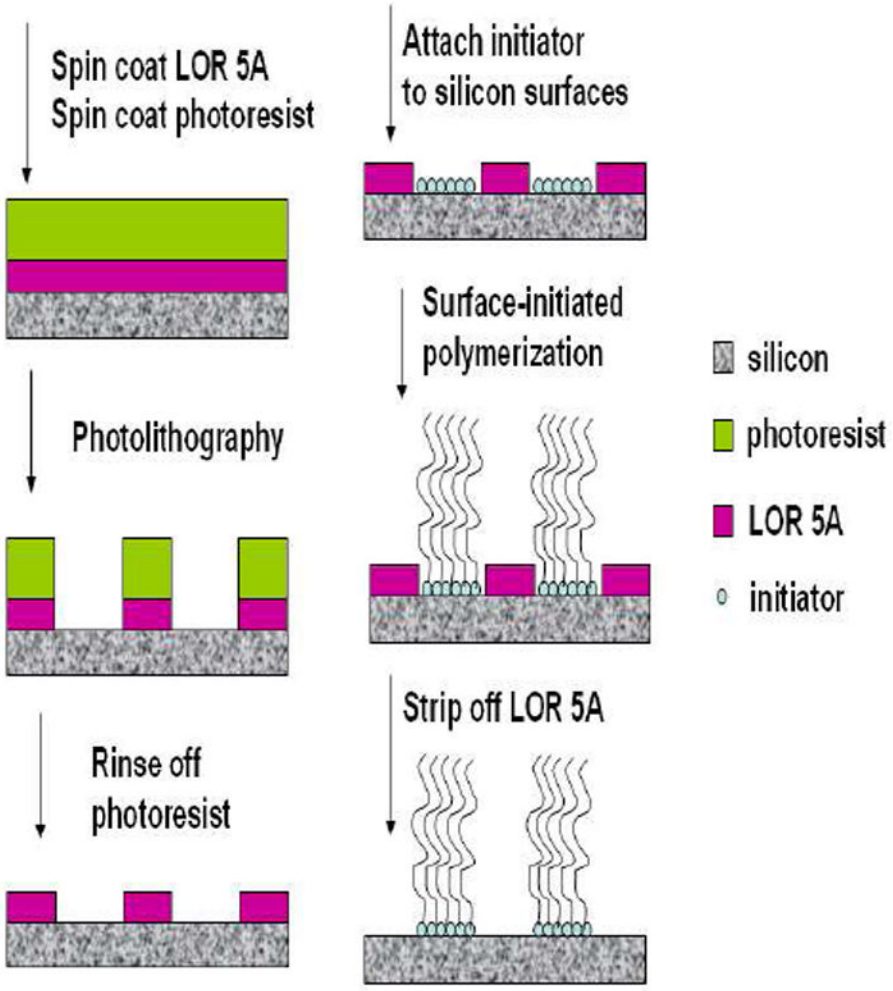

Figure 1.

Patterning of PAA brushes. Lift-off resist and photo resist are sequentially deposited onto a silicon wafer. UV photolithography and subsequent resist development results in pattern transfer of squares (or lines) with dimensions of 1 – 100 μm into the lift-off resist. After attachment of initiator to the silicon surface and subsequent surface-initiated ATRP polymerization, the lift-off resist is removed.

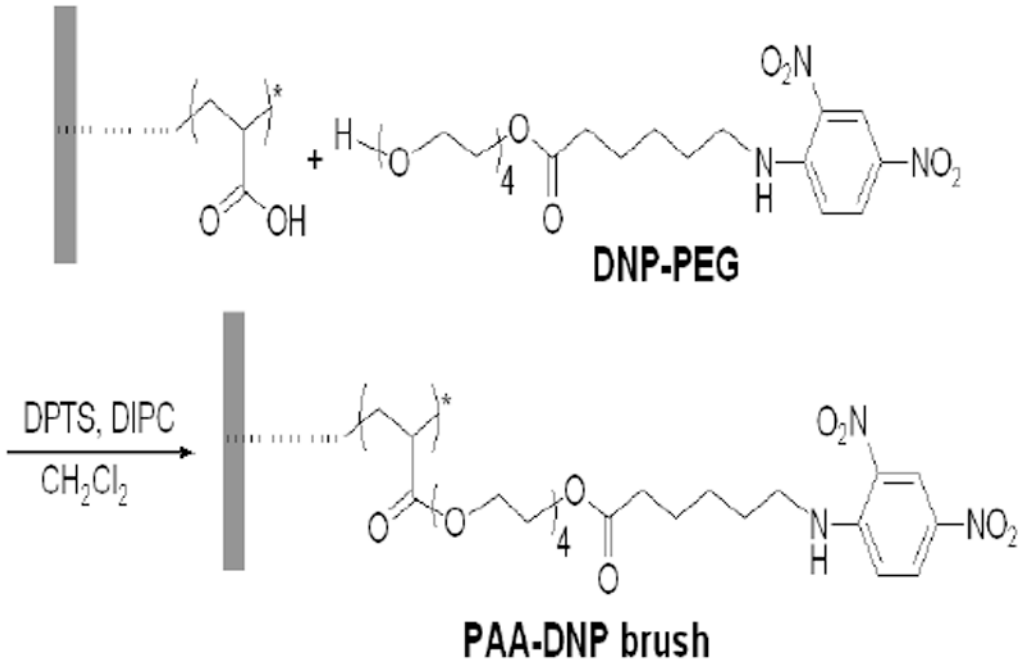

Figure 2.
Modification of patterned PAA brushes with DNP-PEG. Procedure is described in Materials and Methods.

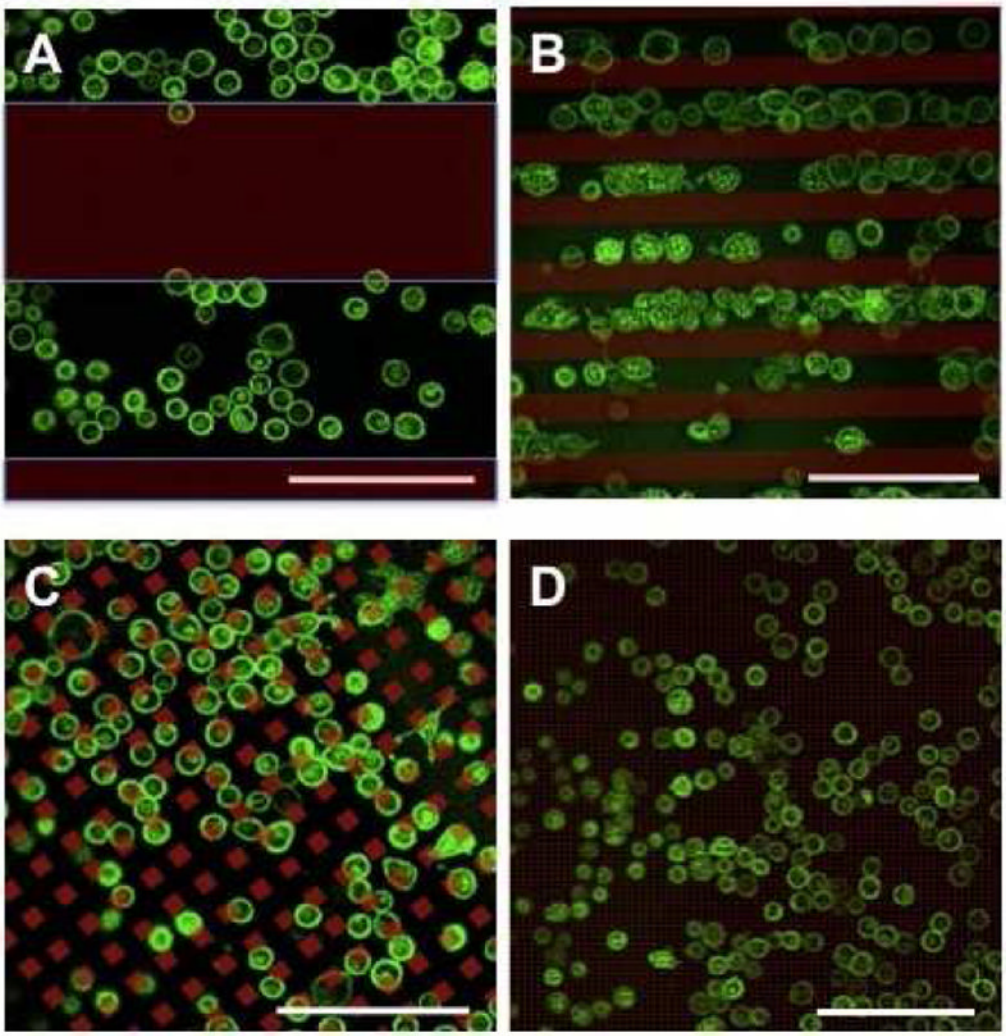

Figure 3.

Cells attach to silicon and spread over small PAA brush features (<10 μm) while avoiding PAA brush regions with large feature sizes (>20 μm). Cells were labeled with A488-IgE (green) and incubated for 20 min at 37°C with 100 μm wide strips (A) 20 μm wide strips (B), 10 μm squares (C), or 2 μm squares (D) of patterned PAA brushes (detected with reflectance and false-colored red). Micrographs are representative of multiple experiments. PAA brush thickness is 30 nm in all cases. Scale bar is 100 μm.

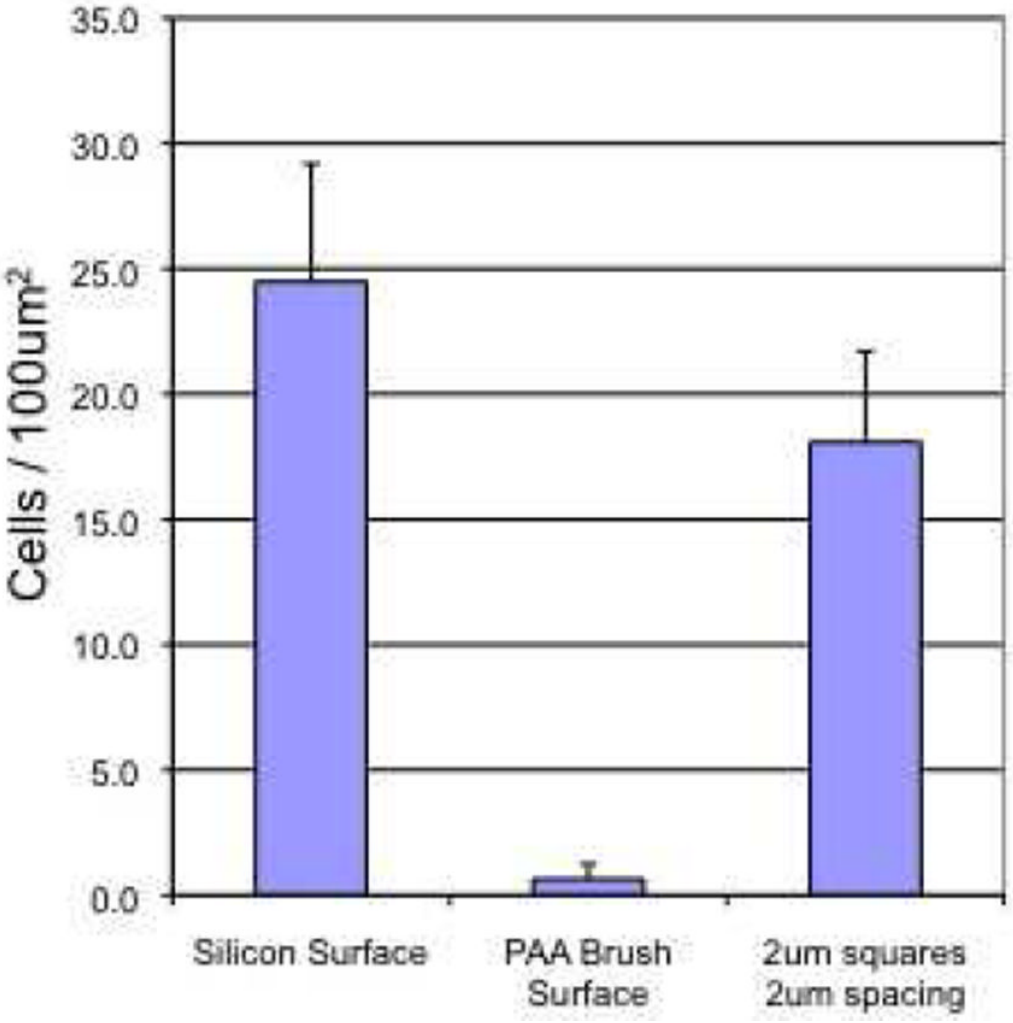

Figure 4.

RBL cells adhere to silicon but not PAA brush coated surfaces unless PAA brushes are patterned with features of subcellular dimensions. Cells (5×10^6/mL were incubated with substrates at 37°C for 20 min prior to gentle wash. Adherent cells, viewed with fluorescence microscopy, were counted and averaged over >10 randomly selected fields of 100 μm^2 in multiple experiments. Error bars show standard deviation.

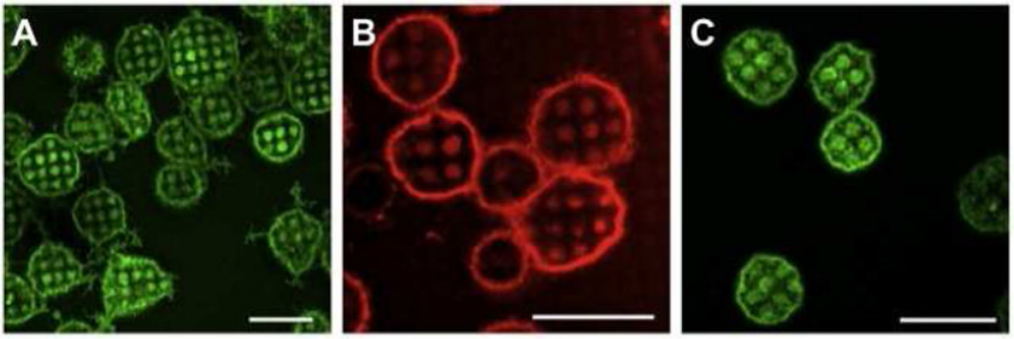

Figure 5.
Cell membrane accumulates over patterned PAA brushes with small feature sizes. Representative fluorescence micrographs of cells incubated with substrates patterned with 2 μm squares of PAA brushes (30 nm thick). Cells were labeled with A488-IgE (A), TR-DPPE (B), or A488-CTxB (C). Scale bar is 20 μm.

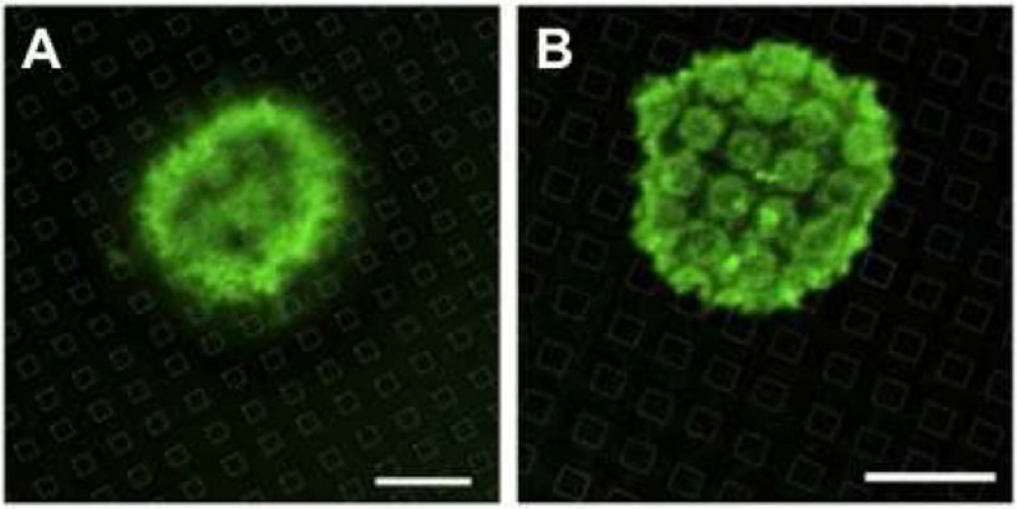

Figure 6.
Membrane accumulates over PAA brushes at 37°C, but much less at room temperature. Representative fluorescence micrographs of cells incubated on surfaces of patterned PAA (30 nm thick) with 2 μm square features for 20 min at room temperature (A) followed by 20 min at 37°C (B). Cells were labeled with A488-IgE. The locations of the PAA features as indicated by light grid lines were determined by reflectance. Scale bar is 10 μm.

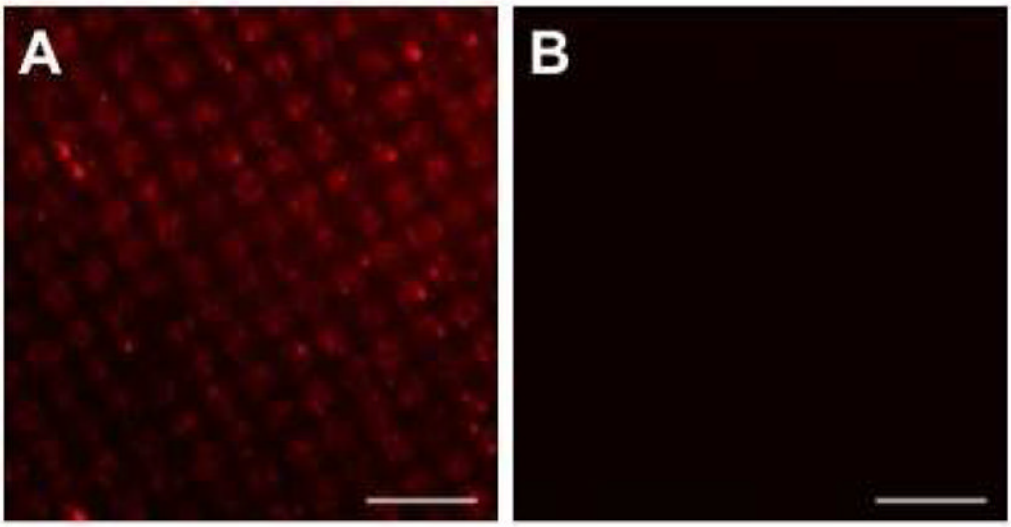

Figure 7.
Fibronectin adsorbs to PAA brushes. Representative fluorescence micrographs show surfaces of patterned PAA (30 nm thick) with 2 μm square features incubated in the presence (A) or absence (B) of fibronectin and visualized with immunofluorescence. Surfaces were treated in parallel with fluorescent antibodies specific for fibronectin. Scale bar is 10 μm.

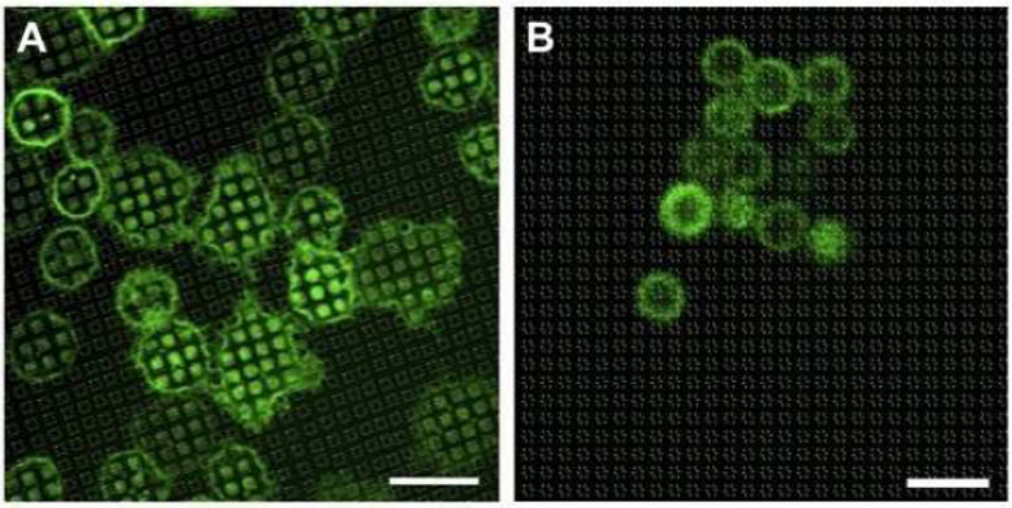

Figure 8.
Inhibition of integrin receptor binding prevents membrane accumulation over PAA brushes. Representative fluorescence micrographs show cells incubated on surfaces patterned with PAA (30 nm thick, 2 μm square features) in the absence (A) or presence (B) of RGD peptides. Cells were labeled with A488-IgE. Locations of the PAA features, as indicated by grid lines, were determined by reflectance. Scale bar is 20 μm.

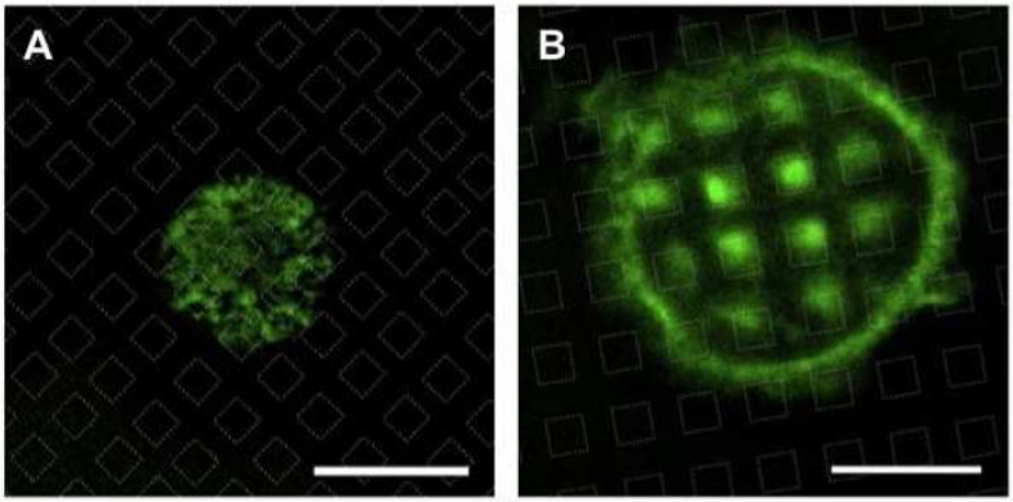

Figure 9.

Actin-EGFP accumulates over patterned PAA brush regions at 37°C, but not at room temperature. Representative fluorescence micrographs show cells expressing actin-EGFP incubated on surfaces patterned with PAA (30 nm thick, 2 μm square features). Cells were incubated with identical substrates for 20 min at room temperature (A) or at 37°C (B). Locations of the PAA features, as indicated by grid lines, determined by reflectance. Scale bar is 10 μm.

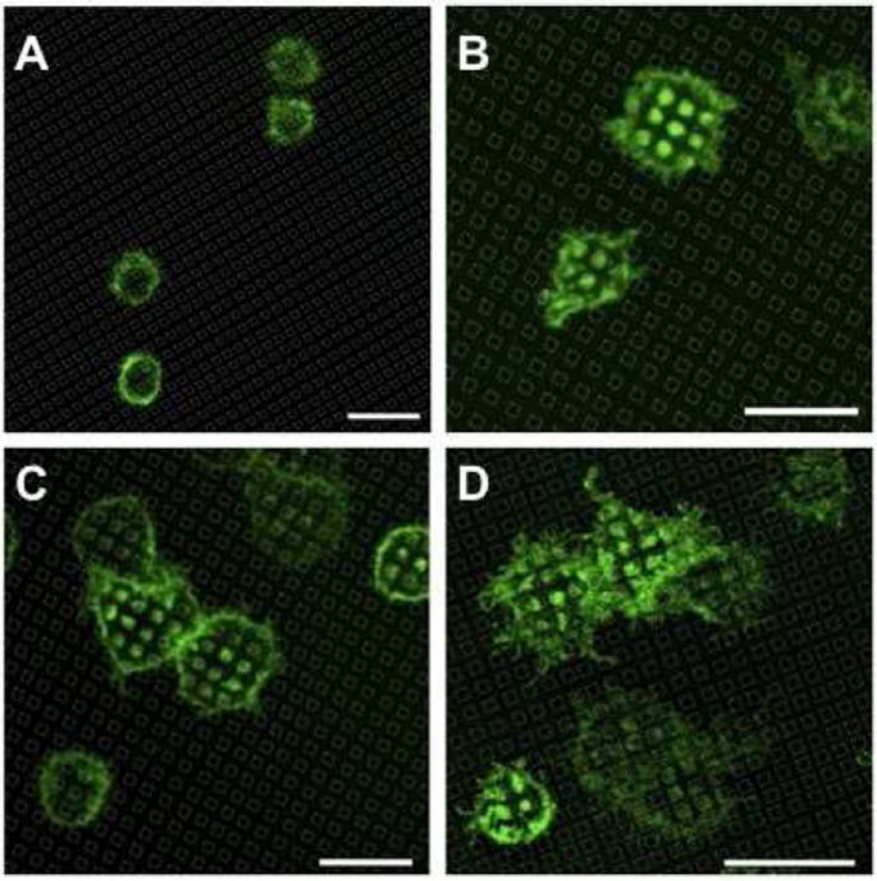

Figure 10.

Cytochalasin D prevents membrane accumulation over patterned PAA regions. Representative fluorescence micrographs show cells sensitized with A488-IgE and incubated on surfaces patterned with PAA (30 nm, 2 μm square features). Cells were pre-treated with Cytochalasin D before incubation with substrates for 20 min (A) before the drug was washed out, and the incubation was continued for 20 min (B). Cells were incubated with substrates for 20 min at 37°C (C) prior to the addition of Cytochalasin D and continued incubation for 20 min (D). Location of the PAA features, as indicated by grid lines, was determined by reflectance. Scale bar is 20 μm.

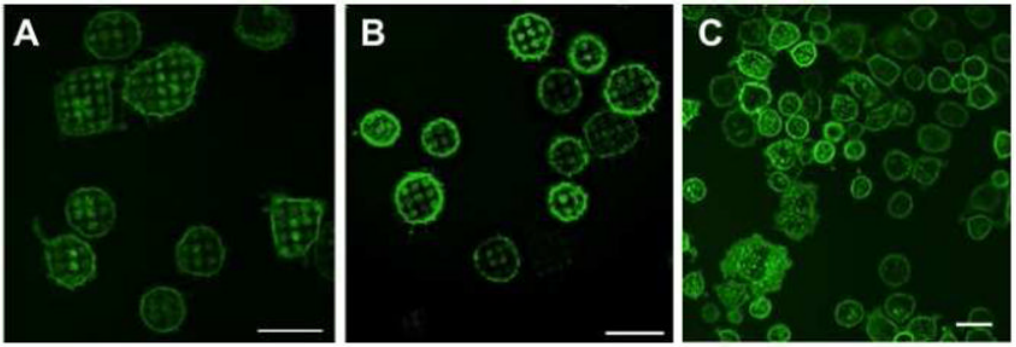

Figure 11.
Membrane accumulates over patterned PAA brushes as a function of brush thickness. Representative fluorescence images of RBL cells sensitized with A488-IgE and incubated for 20 min at 37°C on patterned PAA surfaces with 2 μm square feature sizes. Dry brush thickness is 30 nm (A), 15 nm (B) and 8 nm (C). Scale bar is 20 μm.

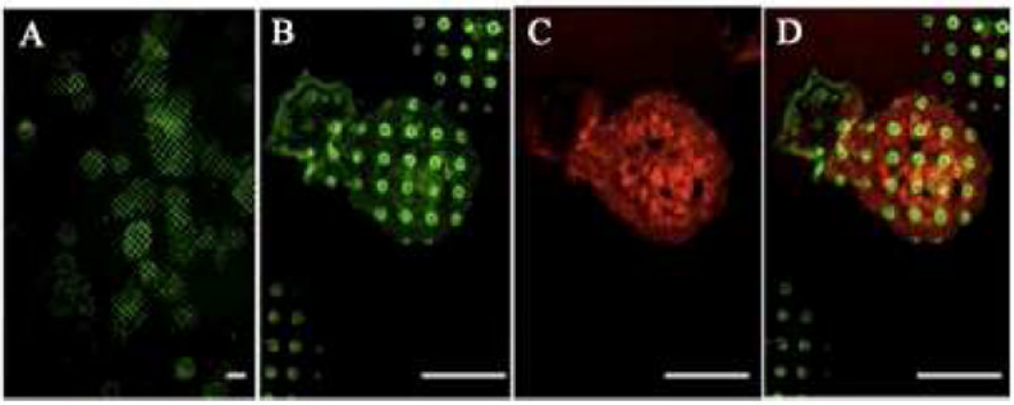

Figure 12.

Patterned DNP-PAA brushes specifically cluster anti-DNP IgE-FcεRI. Cells were labeled with both A488-IgE (green; A, B, C) and $DiIC_{16}$ (red; C, D) and incubated on surfaces patterned with PAA-DNP (8 nm thick, 2 μm squares) at 37°C for 20 min. B, C, D show the same field with green (B) red (C) or merged (D) optics. Scale bar is 10 μm.